SUBSTITUTED APATITE/POLY-EPSILON-CAPROLACTONE BIOCOMPOSITE AS SUBSTRATES AND COATING ON ALPHA-TRICALCIUM PHOSPHATE FOAMS

LE THI BANG

UNIVERSITI SAINS MALAYSIA

2013

SUBSTITUTED APATITE/POLY-EPSILON-CAPROLACTONE BIOCOMPOSITE AS SUBSTRATES AND COATING ON ALPHA-TRICALCIUM PHOSPHATE FOAMS

by

LE THI BANG

Thesis submitted in fulfillment of the requirements for the degree of Doctor of Philosophy

May 2013

ACKNOWLEDGEMENTS

I cherish this chance to express my sincere gratefulness to my supervisor, Prof. Radzali Othman for his support, guidance and inspiration during my period study in USM. His expertise and guidance in combination with his willingness contributed greatly to the advancement of this research project. I am deeply grateful to my advisor, Prof. Kunio Ishikawa at Kyushu University, Japan for his valuable advice and important support throughout this research. I also wish to acknowledge Prof. Do Minh Nghiep and Prof. Tran Quoc Lap for their continuous encouragement and support.

I also wish to express my warm and sincere thanks to the dean, Prof. Hanafi Ismail and all lecturers, administrative and technical staffs in the School of Materials and Mineral Resources Engineering, USM for their continual assistance to accomplish this research. My special thanks are also extended to all the lecturers and staffs in the Department of Dental Science, Faculty of Biomaterials, Kyushu University, Japan for their kindness, help and assistance during my short-term study in Japan. I am grateful to Prof. Ahmad Fauzi Mohd Noor, Prof. Ir. Mariatti Jaafar @ Mustapha, Assoc. Prof. Kanji Tsuru, Assoc. Prof. Masaharu Nakagawa, Maruta-sensei, Dr.Giichiro Kawachi, Dr. Melvin Munar for their sympathetic help and guidance.

I would also like to thank all postgraduate students in School of Materials and Mineral Resources Engineering USM and members of the Prof. Ishikawa' lab for their friendship, in particular, Mr. Shi Xingling, Dr. Alireza Valanezhad from whom I learned most of what I know about cell culture and bone biology. Thanks to all the AUN/SEED-Net students, Nallis, Tram, Nilar, Ila and her family, Farah, Azizul, and

Vietnamese group, Dr. Du Lan, Dr. Viet, Trung, Khang, Duy, Do Quyen for always stay beside me.

Special thanks to ASEAN University Network/Southeast Asia Engineering Education Development Network (AUN/SEED-Net, JICA) for their generosity in giving me this opportunity and financial support to pursue my Ph.D.'s degree.

Finally, I would like to express my deepest gratitude to my family for their constant love, unfailing advice and support. I would like to dedicate all my loving thanks to my father, who made all of this possible and always blessing me. It would be impossible for me to finish this work without my mother loving support over the last couple of years, I never thank her enough. My special gratefulness is due to my lovely husband, Dr. Bui Duc Long, and my son, Bui Thai Son-Bon Bon for their endless love, encouragement and care. Thank you for always be there for me.

Thank you!

LE THI BANG

May, 2013

TABLE OF CONTENTS

ACKNOWLEDGEMENTS ii

TABLE OF CONTENTS iv

LIST OF TABLES x

LIST OF FIGURES xi

LIST OF ABBREVIATION xvii

ABSTRAK xviii

ABSTRACT xx

CHATER 1: INTRODUCTION

1.1 Background 1

1.2 Problem statement 3

1.3 Objective of the research 6

1.4 Project overview 7

CHATER 2: LITERATURE REVIEW

2.1 Introduction 9

2.2 Bone Tissue 10

2.3 Structure of cancellous bone 13

2.4 Scope of tissue engineering 14

2.5 Artificial bone substitutes 15

2.6 Biomaterial 17

2.6.1 Functions and requirements of biomaterials in tissue engineering 19
2.6.2 Calcium phosphate ceramics 21
2.6.2.1 Hydroxyapatite 24
2.6.2.2 Tricalcium phosphate 26
2.6.3 Ionic-substituted apatite 27
2.6.3.1 Carbonate substitution 28
2.6.3.2 Heat-treatment of carbonate apatite 32
2.6.3.3 Silicon substitution 34
2.7 Surface reactive calcium phosphate and biological performance evaluation . 37
2.7.1 In vitro evaluation using simulated body fluid 38
2.7.2 In vitro evaluation using cell culture 40
2.8 Bone cell-artificial bone graft interaction 41
2.9 Calcium phosphate/PCL biocomposite: Biocomposite compound selection . 43
2.9.1 Poly ε-caprolactone (PCL) 46
2.9.2 Calcium phosphate/PCL coating on α-TCP foam 48
2.10 Summary 49

CHAPTER 3: MATERIALS AND METHOD

3.1 Introduction 50
3.2 Preparation of CO_3Ap and Si-CO_3Ap powders 50
3.2.1 Starting materials 50
3.2.2 Synthesis parameters 50
3.2.3 Carbonate apatite (CO_3Ap) 51
3.2.3.1 Effect of different carbonate ion supply on the CO_3Ap formation 52

3.2.3.2 Thermal behavior of CO_3Ap with different carbonate ion supply 53
3.2.4 Silicon substituted carbonate apatite (Si-CO_3Ap) 54
3.3 Fabrication of a porous structured of Si-CO_3Ap/PCL biocomposite 57
3.3.1 Preparation of interconnected porous Si-CO_3Ap 57
3.3.2 Preparation of porous Si-CO_3Ap/PCL biocomposite 58
3.4 CO_3Ap/PCL biocomposite and PCL-coated α-TCP foam 60
3.4.1 Fabrication of α-TCP foam 60
3.4.2 PCL and CO_3Ap/PCL coating on α-TCP foam 61
3.5 Bioactivity evaluation of CO_3Ap and Si-CO_3Ap in vitro: Stimulated Body Fluid (SBF) 64
3.6 In vitro evaluation on the biocompatibility of CO_3Ap, Si-CO_3Ap and CO_3Ap/PCL coated α-TCP: Cell study 64
3.6.1. Sample preparation 64
3.6.2 MC3T3-E1 osteoblast-like cell 65
3.6.3 Rat bone marrow cell isolation 66
3.7 Characterization techniques 66
3.7.1 X-ray Diffraction (XRD) 66
3.7.2 Fourier Transform Infrared (FTIR) spectroscopy 68
3.7.3 Scanning Electron Microscopy (SEM) 68
3.7.4 Transmission Electron Microscope (TEM) 69
3.7.5 Elemental Analyzer (CHN) 69
3.7.6 X-ray Fluorescence (XRF) 70
3.7.7 Density Measurements 70
3.7.8 Inductively Coupled Plasma (ICP) Spectroscopy 72
3.7.9 Diametral Tensile Strength (DTS) 73

3.7.10 Compressive strength 74
3.8 Evaluation of bioactivity and solubility 74
3.9 Cell study evaluations 76
3.9.1 Cell detachment and cell counting prior to seeding on the sample 76
3.9.2 Initial Cell Attachment 77
3.9.3 Cell morphology 78
3.9.4 Cell proliferation 78
3.9.5 Alkaline phosphatase activity 79
3.9.6 Total protein content 81
3.10 Surface roughness measurement 82
3.11 Statistical Analysis 82

CHAPTER 4: RESULTS AND DISCUSSION

4.1 Introduction 83
4.2 Part 1: Carbonate apatite and silicon-substituted carbonate apatite 83
4.2.1 Evaluation of different carbonate ion sources on the synthesis of CO_3Ap 83
4.2.1.1 XRD and FTIR analysis of the as-synthesized CO_3Ap powders 84
4.2.1.2 Physical properties and morphology of the as-synthesized CO_3Ap powders 86
4.2.2 Thermal behavior of CO_3Ap powders in CO_2 atmosphere 88
4.2.2.1 XRD analysis 89
4.2.2.2 FTIR analysis 92
4.2.3 Silicon-substituted carbonate apatite 97
4.2.3.1 Physical and chemical composition analyses 98

4.2.3.2 XRD analysis 100
4.2.3.3 FTIR analysis 103
4.2.3.4 Evaluation of mechanical properties and microstructure 105
4.2.3.5 Solubility evaluation 109
4.2.4 Bioactivity of CO_3Ap and Si-CO_3Ap in vitro: Stimulated Body Fluid (SBF) 112
4.2.5 Cell study in vitro: MC3T3-E1 Osteoblast-like cell 115
4.2.5.1 Initial cell attachment 115
4.2.5.2 Cell morphology and adherence 117
4.2.5.3 Cell proliferation: AlamarBlue assay 120
4.2.6 Cell study in vitro: Rat Bone Marrow Cells (RBMC) 122
4.2.6.1 Cell morphology 123
4.2.6.2 RBMC proliferation: AlamarBlue assay 124
4.2.6.3 RBMC differentiation: Alkaline phosphatase activity (ALP) 126
4.3 Part 2: Fabrication of porous Si-CO_3Ap/poly-ε-caprolactone (PCL) biocomposite 127
4.3.1 Porous structure of Si-CO_3Ap and Si-CO_3Ap/PCL biocomposite 127
4.3.2 Physical and mechanical properties of porous Si-CO_3Ap and the Si-CO_3Ap/PCL biocomposite 132
4.4 Part 3: Fabrication of fully interconnected structure of PCL and PCL/CO_3Ap coated α-TCP foam 136
4.4.1 XRD and FTIR analysis of α-TCP foams 136
4.4.2 Physical properties, morphology and microstructure of the α-TCP specimens 138
4.4.3 Compressive strength and fracture surface morphology 143

4.4.4 Discussion (PCL and CO_3Ap/PCL coated α-TCP foam) 146

4.4.5 Rat bone marrow cell response on different CO_3Ap/PCL coated α-TCP foams 150

4.4.5.1 Initial cell attachment and cell morphology 151

4.4.5.2 Proliferation test 152

4.4.5.3 Alkaline Phosphatase Activity (ALP) 153

4.4.5.4 Discussions (Cell study on different α-TCP foams) 154

CHAPTER 5: CONCLUSION AND RECOMENDATION

5.1 Conclusion 157

5.2 Recommendation for future work 159

REFERENCES 162

APPENDICES 181

LIST OF PUBLICATIONS 190

LIST OF TABLES

Table 2.1 Composition of the human enamel and bone [60] 11

Table 2.2 Mechanical properties of cortical and cancellous bones [55] 13

Table 2.3 Materials for use in the body [76] 19

Table 2.4 Factors influencing degradation rate of calcium phosphate [86] 22

Table 2.5 Calcium phosphates used in tissue engineering [94] 23

Table 2.7 Infrared vibration bands of carbonate groups in calcium phosphate apatite 31

Table 2.8 Property of PCL 47

Table 3.1 Composition and designation of the samples 62

Table 3.2 Ion concentrations of SBF and the human blood plasma [131] 75

Table 3.3 Reagents for the preparation of SBF solution 75

Table 3.4 Amount of working reagents used for ALP measurement 81

Table 4.1 Physical properties of the as-synthesized CO_3Ap powders 87

Table 4.2 Physical and chemical properties of the as-synthesized CO_3Ap and Si-CO_3Ap 98

Table 4.3 CO_3 contents in the CO_3Ap and Si-CO_3Ap samples before and after heat treatment 99

Table 4.4 Lattice parameters and crystallite size of the as-synthesized CO_3Ap and Si-CO_3Ap powders 101

Table 4.5 Surface roughness and crystallite size of samples for cell study 117

LIST OF FIGURES

Fig. 1.1 Flow chart of the research 8

Fig. 2.1 General structure of a mammalian bone 12

Fig. 2.2 Hierarchical structure of bone: (a) selection through a femur head showing the shell of the trabecular (spongy bone) and the cortical (compact bone), (b) SEM image of the cancellous bone showing the high porosity and the interconnecting network of pores (magnification: 40X) 14

Fig. 2.3 The atomic arrangement of calcium hydroxyapatite..... 25

Fig. 2.4 Typical SEM image of osteobclast bone resorption on (a) sintered hydroxyapatite, (b) cortical bone, (c) sintered carbonate apatite 28

Fig. 2.5 Solubility of carbonate apatite in acidic condition as a function of carbonate content 29

Fig. 2.6 SEM image of carbonate apatite after 12 weeks in vivo (a) dissolution of an entire grain at a triple-junction and (b) grain boundary dissolution... 30

Fig. 2.7 SEM images of NaOH- treated on Ti metal: (a) surface, (b) cross-section 39

Fig. 2.8 The time course of osteoblast function on a newly implanted biomaterial 41

Fig. 2.9 Ring opening polymerization of ε-caprolactone to polycaprolactone 47

Fig. 3.1 Flowchart for the synthesis of carbonate apatite..... 52

Fig. 3.2 Flow chart for the synthesis of Si-CO_3Ap and the comparison of CO_3Ap and Si-CO_3Ap 55

Fig. 3.3 Flowchart for preparation of porous Si-CO_3Ap and its characterization 57

Fig. 3.4 Flowchart for the preparation of porous biocomposite 58

Fig. 3.5 Heat-treatment regime for the fabrication of α-TCP foam 61

Fig. 3.6 Figure 3.6 Illustration showing the applied load during a DTS test 73

Fig. 3.7 (a) Bottle used for SBF test and (b) arrangements of specimen in the SBF 76

Fig. 3.8 Counting systems to ensure accuracy and consistency. Count the cells within the large square and those crossing the edge on two out of the four sides. 77

Fig. 4.1 XRD patterns of the as-synthesized CO_3Ap: (a) CO_3Ap-D, (b) CO_3Ap-W, and (c) CO_3Ap-T 84

Fig. 4.2 FTIR spectra of the as-synthesized CO_3Ap powders: (a) CO_3Ap-D, (b) CO_3Ap-W, and (c) CO_3Ap-T 85

Fig. 4.3 TEM images of the as-synthesized CO_3Ap powders: (a) CO_3Ap-D, (b) CO_3Ap-W, and (c) CO_3Ap-T. Scale bar = 100 nm 88

Fig. 4.4 (a) XRD patterns of the CO_3Ap-D from 800-1000^oC: 90

Fig. 4.4 (b) XRD patterns of the CO_3Ap-W from 800-1000^oC 90

Fig. 4.4 (c) XRD patterns of the CO_3Ap-T from 800-1000^oC 91

Fig. 4.5 (a) FTIR spectra of CO_3Ap-D after heat-treatment in wet CO_2 gas 92

Fig. 4.5 (b) FTIR spectra of CO_3Ap-D after heat-treatment in dry CO_2 gas 93

Fig. 4.6 (a) FTIR spectra of CO_3Ap-W after heat treatment in wet CO_2 gas 94

Fig. 4.6 (b) FTIR spectra of CO_3Ap-W after heat treatment in dry CO_2 gas 94

Fig. 4.7 (a) FTIR spectra of CO_3Ap-T after heat treatment in wet CO_2 gas 95

Fig. 4.7 (b) FTIR spectra of CO_3Ap-T after heat treatment in dry CO_2 gas 95

Fig. 4.8 XRD patterns of the as-prepared powders: (a) CO_3Ap and (b) Si-CO_3Ap 100

Fig. 4.9 XRD patterns of the samples after heat-treatment; Si-CO_3Ap at: (a) 650^{o}C, (b) 700^{o}C and (c) 750^{o}C, and CO_3Ap at: (d) 650^{o}C, (e) 700^{o}C and (f) 750^{o}C 102

Fig. 4.10 FTIR spectra of the as-prepared powders: (a) CO_3Ap and (b) Si-CO_3Ap 104

Fig. 4.11 Density of samples after heat-treatment at different temperatures. *p<0.05 and #p<0.05, statistically different compared to CO_3Ap and Si-CO_3Ap heat-treated at 650^{o}C, respectively, n= 106

Fig. 4.12 SEM microstructure of sample after heat-treatment at 700^{o}C: (a) CO_3Ap and b) Si-CO_3Ap (Magnification: 50KX) 106

Fig. 4.13 Diametral Tensile Strength (DTS) of samples heat-treated at different temperatures. *p<0.05 and #p<0.05, statistically different compared to CO_3Ap and Si-CO_3Ap heat-treated at 650^{o}C, respectively, n=8 108

Fig. 4.14 DTS vs. heat-treatment temperatures for various carbonate hydroxyapatites 109

Fig. 4.15 Released ions in SBF solution after immersion: (a) released Ca, (b) released Si 110

Fig. 4.15 (Cont') pH of SBF solution after immersion 111

Fig. 4.16 Typical surface morphology of the specimen before immersion in SBF: (a) CO_3Ap, (b) Si-CO_3Ap. Magnification: 500X 113

Fig. 4.17 SEM images of the surface of CO_3Ap after immersion in SBF for (a) 3 days (Mag. 1KX), (b) 7 days (Mag. 5KX) 114

Fig. 4.18 SEM images of the surface of Si-CO_3Ap after immersion in SBF for (a) 3 days (Mag. 1KX), (b) 7 days (Mag. 5KX) 114

Fig. 4.19 Initial cell attachment of MC3T3-E1 after 4 hours culture: (a) as-synthesized CO_3Ap, (b) as-synthesized Si-CO_3Ap, (c) CO_3Ap-700^oC, (d) Si-CO_3Ap-700^oC 116

Fig. 4.20 Cell morphology after culture for 4 hour: (a), (b): as-synthesized CO_3Ap; (c), (d): as-synthesized Si-CO_3Ap; (e), (f): CO_3Ap-700^oC and (g), (h): Si-CO_3Ap-700^oC. The white arrows indicate the adhered cell..... 118

Fig. 4.21 MC3T3-E1 cells proliferation: (a),(b): as-synthesized CO_3Ap; (c), (d) as-synthesized Si-CO_3Ap; (e), (f) CO_3Ap-700^oC; (g), (h) Si-CO_3Ap-700^oC 119

Fig. 4.22 Cell proliferation of MC3T3-E1 on the different samples..... 121

Fig. 4.23 SEM images of bone marrow cell morphology on: (a) CO_3Ap-700^oC, (b) Si-CO_3Ap-700^oC 123

Fig. 4.24 RBMC proliferation on CO_3Ap-700^oC and Si-CO_3Ap-700^oC 125

Fig. 4.25 ALP activity of RBMC on heat-treated CO_3Ap and Si-CO_3Ap 127

Fig. 4.26 XRD patterns of Si-CO_3Ap powders: (a) as-synthesized Si-CO_3Ap, (b) porous Si-CO_3Ap after heat-treatment at 700^oC 128

Fig. 4.27 Cross-section SEM images of the porous Si-CO_3Ap and Si-CO_3Ap/PCL biocomposite with different wax contents: (a) Si-CO_3Ap-40%, (b) Si-CO_3Ap/PCL-40%, (c) Si-CO_3Ap-60%, (d) Si-CO_3Ap/PCL-60%, (e) Si-CO_3Ap-80% and (f) Si-CO_3Ap/PCL-80%. Magnification 50X 129

Fig. 4.28 Closed porosity of porous Si-CO_3Ap and Si-CO_3Ap/PCL biocomposite versus the wax contents..... 130

Fig. 4.29 Si-CO_3Ap-PCL interphase: (a) Si-CO_3Ap/PCL-40wt%, (b) Si-CO_3Ap/PCL-80wt%. Magnification 200X 132

Fig. 4.30 Void space of porous SiCO_3Ap and Si-CO_3Ap/PCL biocomposite versus the wax contents: (a) initial void space, (b) estimated void space 133

Fig. 4.31 PCL contents of Si-CO_3Ap/PCL biocomposite versus the wax contents 133

Fig. 4.32 Porosity and DTS values of the porous Si-CO_3Ap and Si-CO_3Ap/PCL biocomposite: (a) Porosity, (b) DTS. 135

Fig. 4.33 XRD patterns of (a) standard α-TCP and (b) α-TCP obtain from $CaCO_3$+DCPD, (c) PCL-coated α-TCP and (d) CO_3Ap/PCL-coated α-TCP 137

Fig. 4.34 FTIR spectra of the α-TCP scaffolds before and after coating: (a) α-TCP, (b) α-TCP/PCL, (c) α-TCP/CO_3Ap/PCL, (d) CO_3Ap, (e) PCL 138

Fig. 4.35 Optical macrostructure of foam surface: (a) α-TCP, (b) α-TCP (5), (c) α-TCP (10), (d) α-TCP (15), (e) CO_3Ap/PCL (1/3), (f) CO_3Ap/PCL (2/3),(g) CO_3Ap/PCL (3/3) 139

Fig. 4.36 (a) Coating content and porosity of α-TCP foam coated with PCL at different PCL solution concentrations 140

Fig. 4.36 (b) Coating content and porosity of α-TCP foam coated with CO_3Ap/PCL: (i) CO_3Ap/PCL=1/3, (ii) CO_3Ap/PCL=2/3, (iii) CO_3Ap/PCL=3/3 141

Fig. 4.37 SEM images of α-TCP foams: (a) α-TCP (0), (b) α-TCP (10), (c) CO_3Ap/PCL (1/3), (d) CO_3Ap/PCL (2/3) and (e) CO_3Ap/PCL (3/3) specimens. Magnification 100X..... 142

Fig. 4.38 Cross-section of specimen before and after coating: (a) α-TCP (0), (b) α-TCP (5), (c) α-TCP (10), (d) CO_3Ap/PCL (1/3, (e) CO_3Ap/PCL (2/3), (f) CO_3Ap/PCL (3/3). Magnification 500X 143

Fig. 4.39 Typical stress-strain curve of the foam specimens upon compression test: (a) α-TCP (0), (b) α-TCP (15). 144

Fig. 4.40 Compressive strength of pure α-TCP (Fig. 4.40 (a) at 0%PCL) and coated specimen: (a) with PCL at different PCL solution concentrations, (b) with CO_3Ap/PCL at different CO_3Ap contents: (i) CO_3Ap/PCL (1/3), (ii) CO_3Ap/PCL (2/3), (iii) CO_3Ap/PCL (3/3). 145

Fig. 4.41 Typical fracture struts of (a) α-TCP (0), (b) α-TCP (5), (c) α-TCP (10), (d) α-TCP (15). Magnification 200X 146

Fig. 4.42 Initial cell attachment on different surfaces after 5 h culture: (a) [α-TCP (0)], (b) [α-TCP (10)], (c) [CO_3Ap/PCL (1/3)], (d) [CO_3Ap/PCL (3/3)] 151

Fig. 4.43 SEM images of cell morphology after 5 hours of culture: (a) α-TCP (0), (b) α-TCP (10), (c) CO3Ap/PCL (1/3), (d) CO3Ap/PCL (3/3). Scale bar = 30 µm 152

Fig. 4.44 Number of adherent cells calculated from AlamarBlue activity: (a) α-TCP (0), (b) α-TCP (10), (c) CO_3Ap/PCL (1/3), (d) CO_3Ap/PCL (3/3) 153

Fig. 4.45 ALP activity: (a) α-TCP (0), (b) α-TCP (10), (c) CO_3Ap/PCL (1/3), (d) CO_3Ap/PCL (3/3) 154

LIST OF ABBREVIATION

ALP	: Alkaline Phosphatase
BCA	: Bovine Serum Albumin
CaP	: Calcium phosphates
Ca/P	: Calcium-to-phosphorous molar ratio
CO_3Ap	: Carbonate apatite
Si-CO_3Ap	: silicon-substituted carbonate apatite
TCP	: Tricalcium phosphate
CHN	: Carbon, hydrogen, and nitrogen
DCPD	: Deficient-calcium phosphate dihydrate
DTS	: Diametral Tensile Strength
SEM	: Scanning Electron Microscope
FBS	: Fetal Bovine Serum
PBS	: Phosphate Buffer Saline
FTIR	: Fourier Transform Infra-Red
FWHM	: Full Width at Half Maximum
HAp	: Hydroxyapatite
ICDD	: International Centre for Diffraction Data
ICP	: Inductively coupled plasma
S.G.	: Specific gravity
SBF	: Simulated Body Fluid
TEM	: Transmission Electron Microscope
XRD	: X-ray Diffraction
XRF	: X-ray Fluorescence
α-TCP	: Alpha Tri-Calcium Phosphate
α-MEM	: Alpha minimal essential medium
U/mg protein	: µmol/min/mg protein

BIOKOMPOSIT APATIT TERTUKAR GANTI/POLI-EPSILON KAPROLAKTON SEBAGAI SUBSTRAT DAN SALUTAN KE ATAS BUSA ALPHA-TRIKALSIUM FOSFAT

ABSTRAK

Dalam kajian ini, biokomposit karbonat dan silikon tertukar ganti apatit/poli-epsilon-kaprolakton (CO_3Ap/PCL) dihasilkan untuk digunakan sebagai pengganti tulang biokomposit berliang. Di samping itu, CO_3Ap/PCL juga disalut ke atas busa α-trikalsium fosfat (α-TCP) untuk meningkatkan sifat mekanikal dan biologi serta mencapai struktur tulang cancellous. Apatit karbonat (CO_3Ap) dan silikon tertukar ganti karbonat apatit (Si-CO_3Ap) telah disintesis melalui kaedah pemendakan. Keputusan menunjukkan bahawa ion silikat dan karbonat bersaing untuk menduduki tapak fosfat dan juga memasuki secara serentak ke dalam struktur hidroksiapatit. Si-tertukar ganti CO_3Ap mengurangkan kehabluran serbuk dan menggalak pembebasan ion yang mengakibatkan kelarutan yang lebih baik berbanding dengan CO_3Ap bebas Si. Penggantian serentak silikon dan karbonat didapati mempunyai kesan yang lebih baik pada peringkat awal kelakuan osteoblast (pendampingan dan pembiakan sel) tetapi tidak pada peringkat semasa/akhir (pembiakan dan pembezaan). Penghasilan biokomposit yang diterbitkan daripada Si-CO_3Ap berliang sambung yang diperkukuhkan dengan PCL lebur telah dibangunkan untuk meniru komposisi dan struktur tulang yang ditokok dengan prestasi mekanikal yang lebih/baik. Blok karbonat apatit yang digantikan silikon telah dihasilkan menggunakan lilin sebagai ejen meruap. Si-CO_3Ap berliang sambung yang diperolehi mempunyai keliangan kira-kira 80% dan saiz liang kira-kira 100-200 μm. PCL melitupi dan menembusi liang Si-CO_3Ap berliang untuk membentuk suatu ikatan yang baik dengan Si-CO_3Ap dan ini membawa kepada peningkatan yang ketara kekuatan tegangan lintang dari

0.23 MPa kepada nilai maksimum 2.04 MPa. Walaupun biokomposit berliang ini sedikit sebanyak menepati keperluan tulang biologi, masih wujud satu cabaran besar untuk menghasilkan bahan pengganti tulang ideal yang menepati struktur semulajadi. Suatu struktur yang saling bersambung sepenuhnya perlu dipertimbangkan. Kelakuan mekanikal, mikrostruktur dan tindakbalas sel α-trikalsium fosfat (α-TCP) yang menyaluti busa CO_3Ap/PCL telah dikaji sebagai langkah awal untuk menghasilkan pengganti tulang jenis *cancellous*. Busa α-TCP telah diperolehi dari pada pensinteran $CaCO_3$ dan $CaHPO_4 \bullet 2H_2O$ pada suhu 1500^oC. Ia kemudiannya disalut dengan CO_3Ap/PCL dan struktur bersambung liang tiga dimensi sepenuhnya telah dikekalkan. Salutan CO_3Ap/PCL ke atas busa α-TCP telah terbukti sangat berkesan untuk meningkatkan kekuatan mekanikal dan keliatan busa α-TCP selain mempamerkan kebioserasian yang cemerlang. Sampel α-TCP bersalut mempamerkan keliangan tinggi (80-85%) dengan saiz liang yang besar (500-700μm) yang menepati struktur tulang *cancellous*. Penilaian biologi in vitro menunjukkan bahawa CO_3Ap/PCL yang digunakan dalam salutan meningkatkan dampingan dan pembiakan sel serta menggalakkan aktiviti alkali fosfatas bagi kedua-dua sel MC3T3-E1 sel sumsum tulang tikus.

SUBSTITUTED APATITE/POLY-EPSILON-CAPROLACTONE BIOCOMPOSITE AS SUBSTRATES AND COATING ON ALPHA-TRICALCIUM PHOSPHATE FOAMS

ABSTRACT

In this research, carbonate and silicon-substituted apatite/poly-ε-caprolactone biocomposite were produced to be used as a porous biocomposite bone substitute. Carbonate apatite/poly-ε-caproplactone (CO_3Ap/PCL) was also used to coat on a fully interconnected structure of α-tricalcium phosphate (α-TCP) foam to enhance the mechanical and biological properties, and to mimic the structure of cancellous bone. Carbonate apatite (CO_3Ap) and silicon-substituted carbonate apatite (Si-CO_3Ap) were synthesized by a precipitation method. The results revealed that the silicate and carbonate ions competed to occupy the phosphate site and also entered simultaneously into the hydroxyapatite structure. The Si-substituted CO_3Ap reduced the powder crystallinity and promoted ion release which resulted in a better solubility compared to that of Si-free CO_3Ap. The silicon and carbonate co-substitution appeared to have a better effect on the early stages of osteoblast behavior (cell attachment and proliferation) rather than the immediate/late stages (proliferation and differentiation). The fabrication of a biocomposite derived from an interconnected porous Si-CO_3Ap reinforced with molten poly-ε-caprolactone (PCL) was then developed to mimic the composition and structure of bone coupled with enhanced mechanical performance. Porous silicon-substituted carbonate apatite blocks were produced using wax as a volatile agent. The interconnected porous Si-CO_3Ap obtained has a porosity of about 80% and a pore size of about 100-200 μm. The PCL covered, and penetrated into the pores of, the porous Si-CO_3Ap to form an excellent bonding with Si-CO_3Ap leading to a significant increase in diametral tensile strength

from 0.23 MPa to a maximum of 2.04 MPa. However, although the porous biocomposite meets the requirement of biological bone to some extent, it remains a great challenge to make the ideal bone substitute materials that mimic the natural structures, in which, a fully interconnected structure should be highly considered. The mechanical behavior, microstructure and cell responses of CO_3Ap/ PCL coated α-tricalcium phosphate (α-TCP) foams were studied as an initial step for the fabrication of a cancellous-type artificial bone replacement. The α-TCP foam was obtained by sintering $CaCO_3$ and $CaHPO_4 \bullet 2H_2O$ at 1500^oC. It was then coated with CO_3Ap/PCL and its three dimensional, fully-interconnected porous structure was found to be maintained. CO_3Ap/PCL coating on α-TCP foam was proven to be very effective in increasing the mechanical strength by 25 times and toughening the α-TCP foam, in addition to excellent biocompatibility as proven by bone marrow cell studies. The coated α-TCP specimens exhibited high porosity (80-85%) with large pore size (500-700μm) that mimic the cancellous bone structure. The *in vitro* biological evaluations indicated that CO_3Ap/PCL used for coating improved cellular attachment, accelerated proliferation and resulting in a greater alkaline phosphatase (ALP) activity of both MC3T3-E1 cell-like and rat bone marrow cells.

CHAPTER 1

INTRODUCTION

1.1 Background

The reconstruction of bone defects is a common challenge in the medical and dental fields. At present, the golden standard for the reconstruction of bone defect is the use of autograft and allograft, in which treatment typically focuses on harvesting tissue from one site to another in the same patient (an autograft) or from one individual to another (allograft) [1, 2]. However, there are serious drawbacks with these two techniques. Harvesting autografts is expensive, painful, and limited supply whilst allografts have serious constraints of transplantation due to the possibility of introducing infection or disease from the donor to the patient [1, 3, 4]. Therefore, artificial bone replacement materials appear to be ideal for clinical applications.

Bioceramics made of calcium phosphates (CaP) appear to be very prominent due to the excellent biocompatibility, bone bonding ability, and provide the advantage of chemical composition similarity to natural bone [2, 5, 6]. About 60 wt% of bone is made of hydroxyapatite (HA: $Ca_{10}(PO_4)_6(OH)_2$), and therefore, HA and other calcium phosphates (e.g. tricalcium phosphate (TCP), biphasic calcium phosphate) have been intensively studied as the major component of bone substitute materials [7-11]. Calcium phosphates have the distinct physiochemical advantages of stability, inertness, and biocompatibility [12].

It is well known that the incorporation of carbonate ions has considerable impact on the crystal lattice of apatite structure, and on the mineralization process. Introduction of carbonate ions in HA increases the dissolution rate and could

enhance the osteointegration rate [10,13,14]. Therefore, carbonate-substituted hydroxyapatite or carbonate apatite (CO_3Ap) is a prospective candidate for bone-substitute material in order to mimic the composition of bone tissue. In addition, CO_3Ap is resorbed faster by osteoclasts and replaced with the new bone at a higher rate compared to HA [15].

Apart from carbonate, silicon substitution in apatites had also been reported to enhance and stimulate osteoblast-like cell activity [16], and promotes bone remodeling processes [17]. The solubility was observed to increase with an increase in structural order due to the presence of foreign ions (i.e. CO_3^{2-}, SiO_4^{4-}) [18-20] in the HA structure. In addition, Si substitution is also able to promote ion releases which are essential for the biological processes [21]; nonetheless only a few research have investigated ion release in synthetic fluids [20] and the cell response. Therefore, the development of synthetic HA powders with a fully completed and controlled level of ionic substitutions in the HA lattice is of great importance in order to approach the natural bone.

After obtaining materials which mimicked the chemical composition of bone mineral, the biological performance was considered as another key issue for the application of calcium phosphate (CaP) in tissue engineering [22], in which cell activities are of fundamental importance in ensuring successful osteointegration. This biological response is influenced by the geometry, chemical composition and morphology of a bone-substitute material [2]. In addition, bone substitute materials with porous structure have a strong bonding with mineral bone and provide a

mechanical interlocking caused by ingrowth of bone tissue into the pores [23], and as such, porous CaPs are preferred in clinical application [24].

1.2 Problem statement

Numerous research works had focused on the synthesis of HA biomaterial substituted with single- or multi-ion substitution of CO_3^{2-} [25, 26], Si [19, 27-29], F [8], Fe [30], etc, whereas the substitution of CO_3^{2-} along with other cations in the apatite structure were restricted to the co-substitution of HA with the ionic pair of Mg^{2+}/CO_3^{2-}[9, 31], Sr^{2+}/CO_3^{2-} [32] and Na^{+}/CO_3^{2-} [33]. Although a few research had been carried out on the synthesis of SiO_4^{4-}/CO_3^{2-} co-substitution in HA [21, 34], it is not clearly apparent whether SiO_4 present in the material completely substituted for the PO_4^{3-} in the HA structure, or whether the replacement was partial. It was reported [18] that both CO_3^{2-} and SiO_4^{4-} reduced HA crystallinity, and the structure could host only a limited amount of the two ions before collapsing. Additionally, the final product contained CO_3 and SiO_4, but there was a lack of experimental evidence on the substitution of these ions i.e. the competition evidence between CO_3 and SiO_4 for substituting the PO_4 ions. Recently, an extensive study on the SiO_4 and CO_3 co-substituted HA had been reported [33]. However, the preparation methods were carried out under air atmosphere and used CO_2 from the atmosphere as the CO_2 source, and as such, there was no control of CO_3 substitution level. Thus, the CO_3 ion present could indeed be doped-HA, where the foreign ion is just adsorbed on the surface of the crystals [18]. Moreover, the mechanical properties and cell activity of the ion-substituted HA after heat-treatment were not fully considered.

Against this background, the first part of this research project was to prepare and characterize carbonate apatite and silicon-substituted carbonate apatite by a precipitation method. The result was aimed to provide an accurate understanding of the changes in hydroxyapatite (apatite) caused by the co-substitution of carbonate (CO_3^{2-}) and silicate (SiO_4^{4-}) ions on the structure, solubility of as-synthesized Si-CO_3Ap powders and mechanical properties. Additionally, the biocompatibility was also studied by performing cell attachment, cell morphology, proliferation and differentiation using rat bone marrow cells and MC3T3-E1 osteoblast-like cells on the CO_3Ap and Si-CO_3Ap specimens (as-synthesized and heat-treated compacts).

It was reported that a porous structure of about 50-90% porosity with appropriate pore size is necessary for bone tissue formation [35,36] whilst the interconnected porous structure is important in the early stages of bone regeneration [37], to facilitate the penetration of mesenchymal cells and osteotropic agents into the pores [38]. The pores should be large enough to allow for cell penetration and adhesion, whilst smaller pores allow for nutrients and oxygen diffusion throughout the scaffold [39].

However, the porosity and structural architecture of porous CaPs significantly affect their mechanical properties, where the strength decreases when the porosity increases [40, 41]. It had been shown that the mechanical properties of a ceramic material can be strengthened by the incorporation of a ductile polymer [2,42,43]. Inherently, natural bone is made up of a biological mineral of CaP and about 40wt% of bioorganic polymers (mainly collagen type I) [2, 44], which is accountable for the superior strength and partial elasticity in biological calcified tissues [45]. Therefore,

the consequent strategy is to combine polymers and CaPs to fabricate scaffolds that meet the requirements desired for bone applications. The fabrication of a biocomposite derived from the interconnected porous CaP reinforced with poly-ε-caprolactone (PCL) was then produced to mimic the composition and structure of bone coupled with enhanced mechanical performance.

Although a porous CaP/PCL biocomposite meets the requirement of biological bone to some extent, it remains a great challenge to make the ideal bone substitute materials that mimic the natural structures, in which, a fully interconnected structure should be highly considered. Among many porous calcium phosphate (CaP), CaP foam gained much attention since it has a fully interconnected porous structure, similar to that of cancellous bone, and high porosity of more than 90%. Up to date, hydroxyapatite foam, α-TCP foam, carbonate apatite (CO_3Ap) foam, and biphasic calcium phosphate foam are the CaP foams reported and studied [5-8]. Although fully interconnected porous structure and large porosity are ideal from a biological point of view, it results in limited mechanical strength. Recently, poly (lactic-co-glycolic) acid (PLGA) coating on CO_3Ap foam was reported to be effective in improving the mechanical properties of CO_3Ap foam [9]. However, fabrication of CO_3Ap foam is complex since CO_3Ap is unstable at the high temperatures required for the sintering process. In contrast, α-TCP is stable at high temperature and is also a biodegradable calcium phosphate.

Coating a polymer on a porous calcium phosphate (CaP) is an alternative method to produce scaffolds with good mechanical strength whilst maintaining high porosity and large pore size. On the other hand, CaP was incorporated with the

polymer in order to improve the biocompatibility of the material [43]. This mixture had shown to be more effective for the enhancement of bioactivity [46]. For example, the incorporation of HA in poly-ε-caprolactone (PCL) matrix of the HA/PCL scaffold showed better adhesion, proliferation of fibroblasts and protein adsorption compared to single HA or single PCL controls [47]. Thus, in this research project, the CO_3Ap was hybridized with PCL and coated on the α-TCP foam.

1.3 Objective of the research

This study is focused on the preparation of silicon and carbonate substituted hydroxyapatite/poly-ε-caprolactone biocomposite as substrate and coating on α-tricalcium phosphate foams with high performance properties which can be applied in biomedical technology. Therefore, the main objectives are:

1. To investigate the simultaneous substitution of SiO_4^{4-} and CO_3^{2-} ions into the HA structure in order to obtain a product which is closer in chemical composition to the natural bone. The competition between CO_3^{2-} and SiO_4^{4-} for substituting the PO_4^{3-} ions in the HA structure was also investigated. The aim of the work was also to evaluate the physical and mechanical properties and the solubility, as well as in vitro cell study of the silicon-substituted carbonate apatite as compared to that of carbonate apatite.

2. To mimic the composition and structure of bone coupled with enhanced mechanical performance. The fabrication of a biocomposite derived from an interconnected porous Si-CO_3Ap reinforced with PCL was developed.

3. In order to mimic the porous structure of cancellous bone which is responsible for 88% of the amount of the bone remodeling, the fully interconnected

structure of CO_3Ap/PCL coated α-TCP biocomposite was fabricated. The mechanical properties and in vitro cell culture of the biocomposite was studied

1.4 Project overview

This research work is divided into three parts which will be described in detail in CHAPTER 3. The first part is synthesis and characterization of CO_3Ap and Si-CO_3Ap, in which a precipitation method with the optimized parameters [48, 49] adapted. The precipitation method allows the production of materials with good crystallinity, physiological stability and with the morphological characteristics of the bone tissue. Additionally, this is a low-cost, simple and versatile technique. Separately, during the reactions, the reaction media involves no foreign elements except water, the only by product. The second part is the fabrication of a porous structured Si-CO_3Ap/poly-ε-caprolactone (PCL) biocomposite derived from porous Si-CO_3Ap block and PCL infiltration.

The final part is the use of CO_3Ap/PCL coating on α-TCP foam to produce a fully interconnected porous structure with very high porosity and large pore size to mimic the cancellous bone-type replacement. The coating of PCL is also made as a control. The influence of PCL concentration solution and CO_3Ap content on the mechanical properties as well as cell response was investigated. In summary, the scope of research is presented in Fig. 1.1.

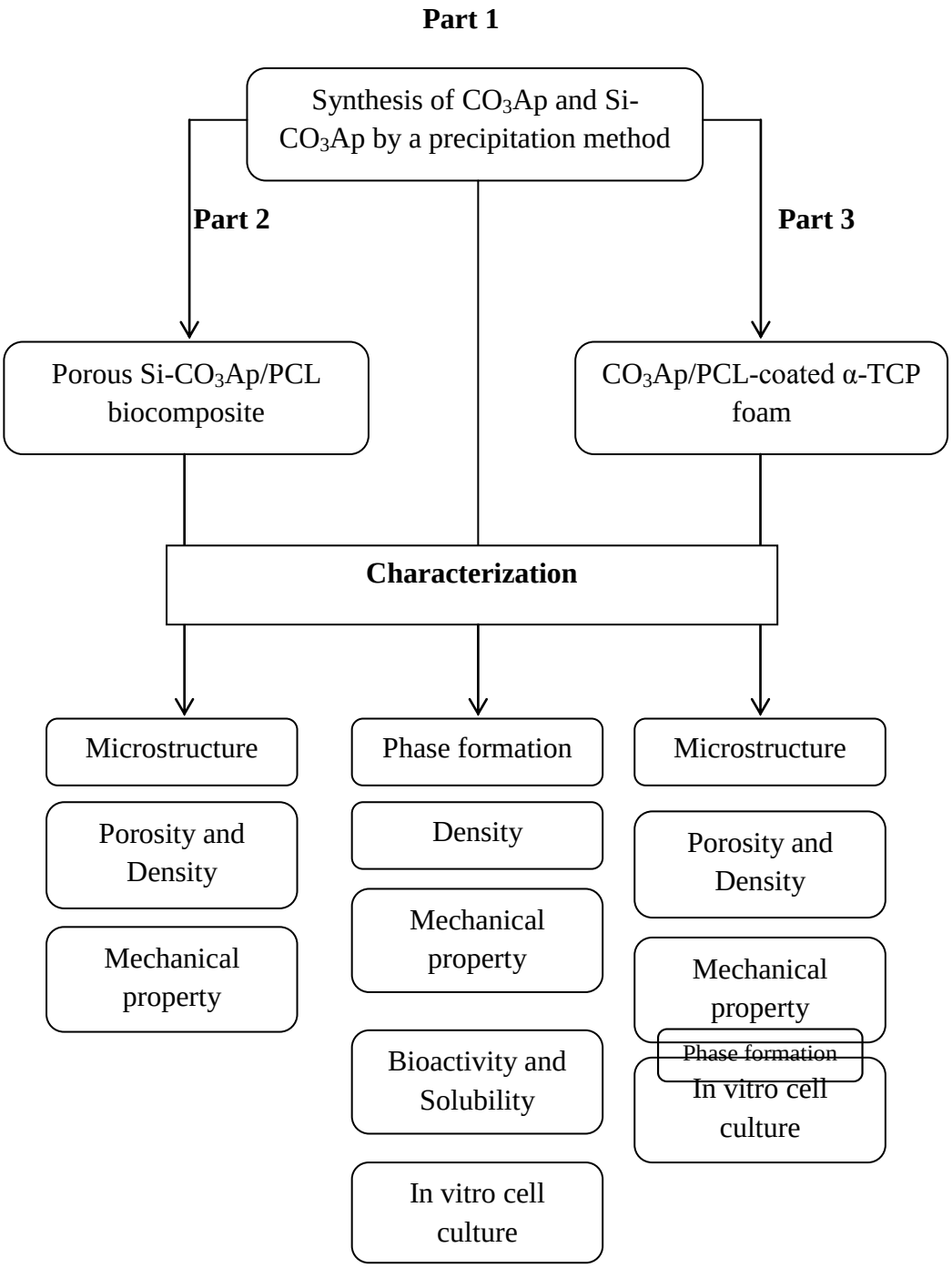

Fig. 1.1 Flow chart of the research

CHAPTER 2

LITERATURE REVIEW

2.1 Introduction

Calcium phosphate ceramics have received considerable attention as artificial bone substitutes because of their excellent tissue compatibility and osteoconductivity [12, 50]. Some of the most commonly used calcium phosphate ceramics are hydroxyapatite (HA) and tricalcium phosphate (TCP) (α and/or β form) [2, 6]. Hydroxyapatite (HA) is the key bioceramic material used for artificial bone substitute because it is found in natural hard tissues as a mineral phase [51]. A remarkable property of the synthetic HA is its excellent bioactivity, which is the ability to form bone bonding after implantation. However, even if the biocompatibility of HA is excellent, the bioactive process in HA shows some shortcomings when compared with other bioactive materials [52], i.e. the bioactivity reactions in silica based glasses take only a few minutes whilst those in HA take several days [29]. In addition, sintered HA have a low solubility rate, and so, it is slowly adsorbed by osteoclast and resulted in a slow replacement by the new bone [15, 53]. In contrast, alpha tricalcium phosphate (α-TCP) is the most soluble compounds among the calcium phosphates. Thus, when fast bone remodeling is desired, α-TCP can be applied.

It is believed that the introduction of carbonate ions and/or silicon ions in the HA would increase its dissolution rate in solution and could enhance its osteointergration rate in vivo [32, 54]. Thus, carbonate apatite (CO_3Ap) and silicon-

substituted carbonate apatite (Si-CO_3Ap) are the other prospective materials for the preparation of bone substitute materials.

Although calcium phosphate (CaP) ceramics have received wide attention for biological applications due to their high bioactivity and osteoconductivity [5, 18], the applications of CaPs have been limited due to their inherent brittleness, low elasticity and low fracture toughness [2]. In addition, the biological performance is another key issue for the application of CaP in clinical uses [22], in which cell activities are of fundamental importance in ensuring successful osteointegration. This biological response is influenced by the geometry, chemical composition and morphology of a bone-substitute material [2]. For a compact, synthetic CaP, only the surface is in contact with the tissue. Thus, porous CaPs are preferred in clinical applications [24].

This review will provide an overview of bone structures, bone cells in bone remodeling processes, as well as the use of biomaterials in tissue engineering. Particularly, bioceramic materials, as a part of biomaterials, will be discussed in more detail in this review. Material selection of biocomposite will also be explained. The final part of this review will address the cell-material interactions, and some evaluation techniques on the biological performance of materials are briefly explained.

2.2 Bone Tissue

Bone is one of the most complex constituents of the body and this is due to the multiple functions that it has to perform [5]. It is a living material composed of cells and a blood supply covered by a strong, interwoven composite structure [55].

The composite is formed by an organic matrix (30wt% of collagen type I) and inorganic mineral nanocrystals of an apatite phase (70t%). The inorganic phase of bone is composed of an impure version of hydroxyapatite, in which carbonate (3-8 wt%) and other ions i.e. $Si^{4+,}$ Na^{+}, Mg^{2+}, K^{+}, F^{-}, Cl^{-}, etc are substituted into its structure [9,10, 27,56,57]. This mineral component gives rise to the compressive strength of bone whilst the organic component is responsible for bone toughness and plasticity [2,58,59]. Table 2.1 shows the comparative composition of human enamel and bone.

Table 2.1 Composition of the human enamel and bone [60]

Constituent	Bone (wt%)	In enamel (wt%)
Calcium, Ca^{2+}	24.50	36.00
Phosphorus, P^{3+}	11.50	17.70
Ca/P molar ratio	1.65	1.62
Sodium, Na^{+}	0.70	0.50
Potassium, K^{+}	0.03	0.08
Magnesium, Mg^{2+}	0.55	0.44
Carbonate, CO_3^{2-}	5.80	3.20
Fluoride, F^{-}	0.02	0.02
Chloride, Cl^{-}	0.10	0.30
Silicon, Si^{4+}	0.003	0.04

In addition, bones are also involved with blood cell formation, calcium metabolism and act as a mineral storage. Bone also contains bone-forming cells (osteoblasts) and bone-resorbing cells (osteoclasts) with various growth factors and molecules [61]. Bone provides the cells in the marrow that differentiates into blood cells, providing mechanical support for the soft tissue and serving as an anchor for the muscles that generate motion [62].

The major support bones consist of an outer layer of cortical (or compact) bone (density ≈ 1.80 g/cm^3) covering an internal spongy structure of cancellous bone, which has a porosity of 75-95 % and a density of about 0.2 g/cm^3 [58, 59, 63] (Fig. 2.1). The porosity reduces the strength of bones but also reduces their weight. Bone architectural properties (cortical thickness, porosity, level of mineralization and properties) derived from the organic phase of bone influenced the load bearing ability of bone [59].

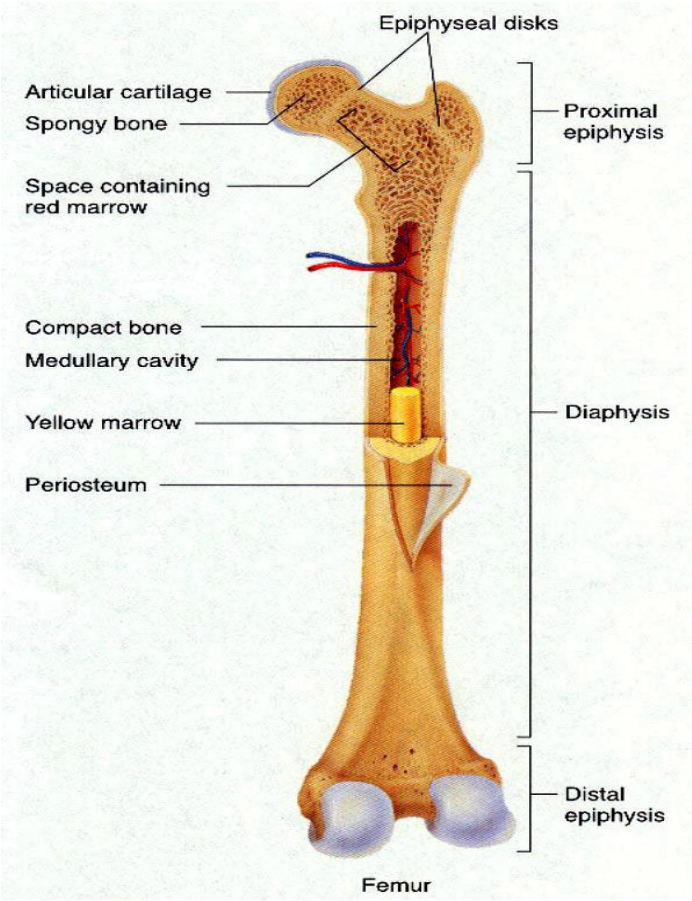

Fig. 2.1 General structure of a mammalian bone [59]

There are some critical physical and chemical characteristics of bone including: (i) interconnected porosity; (ii) biodegradability (remodeling); (iii) bioactivity; (iv) osteoconductivity and (v) osteoinductivity. Pore size in normal

cortical bone ranges from 1 to 10 μm, and 200-400 μm in the trabecular bone. In order to promote bone formation, repair or regeneration, the size and interconnection of the porosity is critical for the diffusion of nutrients, cell attachment, migration, proliferation and differentiation [61].

Differences in mechanical properties depend on the compartment of bone (cortical vs. trabecular bone) as well as the bone orientation. Cancellous bone has a lower modulus of elasticity and a higher strain to failure than a cortical bone [55]. The primary function of trabecular bone (cancellous bone) is to direct stresses to the denser cortical bone [64]. Table 2.2 gives some information about the mechanical properties of bone tissues.

Table 2.2 Mechanical properties of cortical and cancellous bones [55]

Property	**Cortical**	**Cancellous**
Compressive strength (MPa)	100-230	0.1-30
Tensile strength (MPa)	50-150	10-20
Strain to failure	1-2	5-7
Young's Modulus (GPa)	7-30	0.01-2

2.3 Structure of cancellous bone

80% of bone is comprised of dense cortical bone but the cancellous bone is responsible for 88% of the amount of the normal bone remodeling, mainly due to its macroporosity (100μm<pores<1500μm) [65].

Cancellous bone consists primarily of lamellar bone, arranged in packets that make up an interconnected irregular array of plates and rods, called trabeculae (Fig. 2.2). The morphology of a trabeculae material is commonly described as an anisotropic composite of hydroxyapatite, collagen, water and trace amounts of other proteins [66]. The pore is filled with bone marrow. The percentage volume of water, inorganic and organic phases for hydrated trabeculae have been reported at 27%, 38% and 35%, respectively [67]. The orientation of the trabeculae is affected by the mechanical stress to which the bone is subjected to.

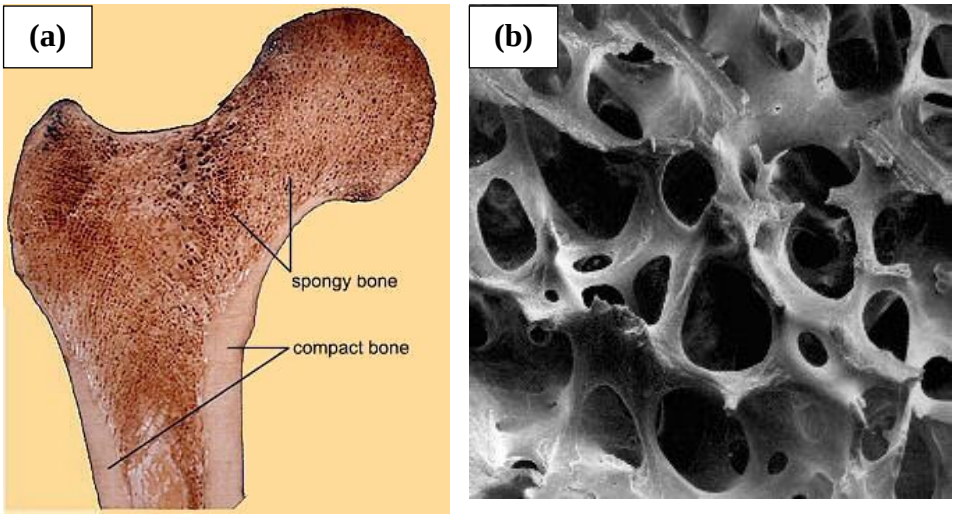

Fig. 2.2 Hierarchical structure of bone: (a) selection through a femur head showing the shell of the trabecular (spongy bone) and the cortical (compact bone), (b) SEM image of the cancellous bone showing the high porosity and the interconnecting network of pores (magnification: 40X)

2.4 Scope of tissue engineering

Most tissues are unable to regenerate when injured or diseased. Even tissues that are able to regenerate spontaneously may not completely do so in large defects. Therefore, tissue engineering has become promising alternative therapy in which organs or tissues can be repaired, replaced, or regenerated [69]

Tissue engineering involves the development of a new generation of materials or devices capable of reconstruction or integration with biological tissues [69]. The cells are central to the regenerative process of any musculoskeletal tissue. They must ultimately be capable of integrating into the host tissue and synthesizing appropriate extracellular matrix. Osteoblasts not only play a central role in bone formation by synthesizing multiple bone matrix proteins, but regulate osteoclast maturation by soluble factors and cognate interaction, resulting in bone resorption [70]. The biomatrix or a bone substitute material used in tissue engineering must have several functions, including a delivery vehicle for the cells or bioactive factors, acts as a template for tissue regeneration [71].

It is needed to distinguish between cell therapy (also called as regenerative medicine) and tissue engineering. Cell therapy is to inject cell to the patient and allow it to grow and differentiate without the assistant of a matrix material or scaffold for medical treatment. Tissue engineering, however, is to provide a guiding and scaffolding framework for cells to adhere to, expand, differentiate, and produce matrices for new tissue formation [69]. Therefore, tissue engineering is especially useful in cases where the lost tissues or organs are three-dimensional, bulky complex structure that cell therapy alone is not effective as a cure because it difficult to control the colonization of transplanted cells [69, 72].

2.5 Artificial bone substitutes

The development of new artificial materials for the repair of bone defects is a great challenge for orthopedic and dental surgery. In order to overcome the limited service lives of implant devices, the emphasis in the development of bone substitutes

is now redirected from bone replacement towards bone tissue regeneration [73]. Numerous artificial bone substitutes are produced from a variety of biomaterials. When determining the suitability of a scaffold for use in tissue engineering, a number of key considerations are important:

(i) Biocompatibility

Biocompatibility is the very first criterion of any scaffold for tissue engineering. The ideal scaffolds should have an appropriate surface chemistry and microstructures to facilitate cellular attachment, proliferation and differentiation [71]. After implantation, the scaffold should elicit a negligible immune reaction in order to prevent it causing a severe inflammatory response that it might reduce healing or cause rejection by the body [1].

(ii) Biodegradability

One of the scopes of tissue engineering is to allow the cells, over time, to eventually replace the implanted scaffold, i.e. to produce a new bone [74]. Thus, the substitute materials must be biodegradable so that the cells can be absorbed to produce their own extracellular matrix. The by-product of this degradation process must be non-toxic or cause inflammatory response to other organs.

(iii) Mechanical properties

Ideally, the scaffold must be strong enough to allow surgical handling during implantation. The scaffolds must have a sufficient mechanical support to function from the time of implantation to the completion of the remodeling process [50]. In

order to support bone ingrowth, the scaffold should not only be osteoconductive but also have adequate mechanical properties to provide initial stability [74].

(iv) Scaffold architecture

The architecture of scaffolds used for tissue engineering is of critical importance [1]. Since bone is a porous tissue material, there is a physiological rationale for the use of porous scaffold in its replacement of bone defects [75]. A bone graft substitute is a fully interconnected porous structure that acts as a template for the bone ingrowth. It was reported that a porous structure of about 50-90% porosity with appropriate pore size is necessary for bone tissue formation [35, 36] whilst the interconnected porous structure is important in the early stages of bone regeneration [37], to facilitate the penetration of mesenchymal cells and osteotropic agents into the pores [38]. The pores should be large enough to allow for cell penetration and adhesion, whilst smaller pores allow for nutrients and oxygen diffusion throughout the scaffold [39].

2.6 Biomaterial

Biomaterial is a term used to indicate materials that constitute parts of medical implants, extra-corporeal devices and disposables that have been utilized for implantation within, or incorporation with, a living system to supplement or replace functions of living tissue or organs [76, 77]. The most commonly used term to describe appropriate biological requirements of a biomaterial is biocompatibility. Biomaterial devices used in orthopaedics are commonly called implants. As a simple definition, biomaterial can be defined as a synthetic material suitable for implanting in a living body to repair damaged or diseased parts [72].

The selected biomaterial should be biodegradable and bioresorbable to support the reconstruction of a completely normal tissue without inflammation. The degradation products must be removed from the body via metabolic pathways [72]. The success of biomaterial in the body depends on factors such as the material properties, design and biocompatibility of the material used [78]. Biomaterials provide a cell-adhesion substrate and can be used to achieve cell delivery with good loading and efficiency to specific sites in the body [79].

The biomaterials should provide adequate mechanical support sufficient to withstand in vivo forces exerted by the surrounding tissue and maintain a potential space for tissue development [72, 80], such as strength, stiffness and fatigue.

Biomaterials can broadly be classified as biological biomaterials (soft and hard tissue type) and synthetic biomaterials (metallic, polymeric, ceramic and composite materials). Each type of synthetic biomaterial has advantages and disadvantages in properties as well as processibility. Metallic biomaterials have mechanical reliability that other biomaterials could not be obtained. Ceramic biomaterials have excellent biocompatibility upon implantation in the body whereas polymeric materials are easy to manufacture to produce various shapes with desired mechanical and physical properties. Some examples of biomaterials are provided in Table 2.3.

Table 2.3 Materials for use in the body [76]

Material	Advantages	Disadvantages	Examples
Polymer (nylon, silicone rubber, polyester, polytetrafuoroethylene, etc.)	Resilient Easy to fabricate	Not strong Deform with time May degrade	Sutures, blood vessels, hip socket, ear, nose, other soft tissues, sutures
Metals (Ti and its alloys, Co-Cr alloys, stainless steels, Au, Ag, Pt, etc.)	Strong, tough, ductile	May corrode, dense, difficult to make	Joint replacements, bone plates and screws, dental root implants, pacer and suture wires
Ceramics (aluminum oxide, calcium phosphates including hydroxyapatite, carbon)	Very biocompatible, inert, strong in compression	Brittle, not resilient, difficult to make	Dental; femoral head of hip replacement, coating of dental and orthopedic implants
Composites (carbon-carbon, wire or fiber reinforced bone cement)	Strong, tailor-made	Difficult to fabricate	Joint implants, heart valves

2.6.1 Functions and requirements of biomaterials in tissue engineering

In tissue engineering, biomaterials replicate the biologic and mechanical functions of the native extracellular matrix (ECM) found in body tissues by serving as an artificial ECM.

Since the majority of mammalian cell types are anchorage dependent, the cell will die if there is no substrate for adhesion. Biomaterial provides a substrate that bone cell can adhere and deliver cells to specific sites in the body with high loading efficiency [81]. Biomaterial can also serve as a cell delivery vehicle, as a drug carrier, to activate specific cellular function in a localized region, and as a barrier

membrane to provide space for tissue regeneration along with the prevention of fibroblast ingrowth into the space [69].

Depending on the tissue sites as well as the applications, there are different requirements for mechanical properties of the biomaterials. The properly chosen biomaterial should allow the engineered tissue to maintain sufficient mechanical integrity to support itself in early development, while in late development it should begin degradation such that it does not hinder further tissue growth [82].

Degradation and absorption of biomaterial are essential in functional tissue regeneration, unless the application is aimed at long term encapsulation of cell to be immunologically isolated. Ideally, the rate of scaffold degradation should mirror the rate of new tissue formation or be adequate for controlled release of bioactive molecules [69]. Furthermore, the biomaterial should provide an environment in which appropriate regulation of cell behavior (e.g., adhesion, proliferation, migration, and differentiation) can occur such that functional tissue can form [81].

Therefore, biomaterials that are intended for use as tissue engineering templates must exhibit several general requirements (i.e. biocompatibility, degradability, osteoconductivity, and mechanical integrity) [83], in order to efficiently perform the function for which they are designed for. The final application of the materials will dictate the type of tissue engineering approach to use and consequently the type of construct needed.

2.6.2 Calcium phosphate ceramics

Calcium phosphate-based bioceramics have been in used in medicine and dentistry for nearly 20 years. Applications include coating of orthopedic and dental implants, maxillofacial surgery, and scaffolds for bone growth and as powders in total hip and knee surgery [84].

Synthetically prepared calcium phosphates are chemically similar to the mineral phase of natural bone tissue, which is a carbonated, calcium-deficient impure hydroxyapatite [10, 56, 85]. Many different biocompatible calcium phosphate species may be prepared to participate actively in the bone remodeling process, although only those that have a molar calcium-to-phosphorous ratio equal to or greater than 1.0 have been reported to be biocompatible and acceptable for use in physiological applications [86].

Calcium phosphate has been synthesized and used for manufacturing various forms of implants, as well as for solid or porous coatings on other implants. There are mono-, di-, tri-, and tetra-calcium phosphates, in addition to the hydroxyapatite and β-whitlockite, which have ratios of 5/3 and 3/2 for calcium and phosphorus (Ca/P), respectively. The stability in solution generally increases with increasing Ca/P ratios [5, 87, 88]. Different phases are used in different applications depending upon whether a degradable or a bioactive material is desired [89].

The stable phases of calcium phosphate ceramics depend considerably upon temperature and the presence of water, either during processing or in the use environment. At body temperature, only two calcium phosphates are stable in contact

with aqueous media, such as body fluids; at pH < 4.2, the stable phase is calcium hydrogen phosphate dehydrate (DCPD: $CaHPO_4 \bullet 2H_2O$ or brushite, C_2P), whereas at pH ≥ 4.2, the stable phase is hydroxyapatite (HA: $Ca_{10}(PO_4)_6(OH)_2$) [90]. At higher temperatures, other phases, such as tricalcium phosphate (TCP: $Ca_3(PO_4)_2$ or C_3P) and tetracalcium phosphate ($Ca_4P_2O_9$) are present. The unhydrated, high-temperature calcium phosphate phases interact with water, or body fluids at 37°C to form HA. Thus, the solubility of a TCP surface approaches the solubility of HA and decreases the pH of the solution which further increases the solubility of TCP and enhances resorption [91].

The rate of dissolution increases as the calcium to phosphorus ratio drops. Hence, tricalcium phosphate resorbs faster than HA. Tricalcium phosphate has four forms; α, β, γ and super α. However, the most commonly used forms for medical applications are the α and β forms. The α-TCP phase crystallizes into a monoclinic space group with a theoretical density of 2.863 g/cm^3. The β-TCP phase has a rhombohedral structure and a theoretical density calculated to be 3.067 g/cm^3 [86]. Research has shown that the α form dissolves at a faster rate than β-TCP. Animal studies have demonstrated that the α form degraded significantly more quickly than the β form after 4 weeks following implantation [92]. Other factors that influence the degradation rate of calcium phosphates are summarized in Table 2.4.

Table 2.4 Factors influencing degradation rate of calcium phosphate [86]

Directly Proportional	**Inversely Proportional**
Increasing surface area	Crystallinity
Substitution: CO_3^{2-}, Mg^{2+}, Si, Sr^{2+} (in HA)	Crystal perfection
	Grain size
	Substitution: F^-, Mg^{2+} (in β)
	Ca:P ratio

Precipitation method is commonly used to fabricate synthetic calcium phosphate. Starting powders can be made by mixing into an aqueous solution the appropriate molar ratios of calcium and phosphate sources which yield a precipitate of stoichiometric HA. The Ca^{2+}, PO_4^{3-} and OH^- ions can be replaced by other ions during processing or in physiological surroundings; e.g., fluorapatite and carbonated apatite. Flourapatite is found in dental enamel and carbornated apatite is present in bone [84].

Depending on the final firing conditions, the calcium phosphate can be hydroxyapatite or β-TCP. In many instances, however, both type of structure exist in the same final product. Several types of CaP biomaterials (Table 2.5) differing in origin, composition and physical forms like particulates or blocks, coating on dental and orthopaedic metal implant are used in maxillo-facial contruction; ear implant; bone repair and augmentation [90, 93].

Table 2.5 Calcium phosphates used in tissue engineering [94]

Name and chemical formula	Ca/P molar ratio	Abbreviation	Type of materials and utilization
Hydroxyapatite $Ca_{10}(PO_4)_6(OH)_2$	1.67	HA	ceramics, plasma sprayed coatings, composites, drug carrier
Calcium deficient apatites	<1.67	ns-HA	low temperature coating composites, drug carrier
α and β tricalcium phosphates $Ca_3(PO_4)_2$	1.50	α and β TCP	cements
Dicalcium phosphate dihydrate $CaHPO_4•2H_2O$	1.0	DCPD	cements, coating
Anhydrous dicalcium phosphate $CaHPO_4$	1.0	DCPA	cements, coating

Table 2.5 (Cont.) Calcium phosphates used in tissue engineering

Name and chemical formula	Ca/P molar ratio	Abbreviation	Type of materials and utilization
Octocalcium phosphate $Ca_8(PO_4)_4$ $(HPO_4)_2$, $5H_2O$	1.33	OCP	cements, bone graft
Tetracalcium phosphate $Ca_4(PO_4)_2O$	2.0	TTCP	cements, drug carrier low temperature coating
Amorphous calcium phosphate	1.5-3.0	ACP	cements, drug carrier low temperature coating
Biphasic calcium phosphate	1.55-1.66	BCP HA/β-TCP	bonegraft, coatings
Fluorapatite, $Ca_{10}(PO_4)_6F_2$	1.67	FA	bonegraft, coating
Carbonated hydroxyapatite $(Ca,Na)_{10}(PO_4,CO_3)_6(OH)_2$	1.7-2.6	CHA	bonegraft

2.6.2.1 Hydroxyapatite

Hydroxyapatite (HA) is the most important among the calcium compounds since it is found in natural hard tissues as a mineral bioceramic phase. Among the most interesting properties of hydroxyapatite as a biomaterial is its excellent biocompatibility. It appears to form a direct chemical bond with hard tissue. In addition, hydroxyapatite acts as a reinforcement in hard tissues and is responsible for the stiffness of bone, dentine, and enamel [77].

According to Park and Lake [95], the mineral part of bone and teeth is made of a crystalline form of calcium phosphate similar to hydroxyapatite. The apatite family of mineral crystallizes into hexagonal rhombic prisms, with the space group being $P6_3/m$ and has unit cell dimensions a = 9.432 Å and c = 6.875 Å. The unit cell contains a complete representation of the apatite crystal, consisting of Ca^{2+}, PO_4^{3-}, and OH^- groups closely packed together in arrangement shown in Figure 2.3. The hydroxyl ions lie on the corners of the projected basal plane and they occur at an